A novel similarity-based status characterization methodology for gear surface wear propagation monitoring

Ke Feng[1], Qing Ni[2,*], Michael Beer[3,4,5], Haiping Du[6], Chuan Li[7]

1. *School of Engineering, University of British Columbia, Kelowna V1V 1V7, Canada*
2. *School of Mechanical and Mechatronic Engineering, University of Technology Sydney, Ultimo, NSW 2007, Australia*
3. *Institute for Risk and Reliability, Leibniz Universität Hannover, Hannover, Germany*
4. *Institute for Risk and Uncertainty, University of Liverpool, Liverpool, United Kingdom*
5. *International Joint Research Center for Resilient Infrastructure & International Joint Research Center for Engineering Reliability and Stochastic Mechanics, Tongji University, Shanghai, China*
6. *Faculty of Engineering and Information Sciences, University of Wollongong, Wollongong, NSW 2522, Australia*
7. *College of Mechanical Engineering, Dongguan University of Technology, Dongguan, PR China*

**corresponding author: qing.ni@outlook.com.au*

Abstract

The gearbox is a vital component for rotating machinery and has been used in many critical engineering applications. Surface wear is a common but inevitable phenomenon during the lifespan of the gearbox. Its propagation can result in some catastrophic failures and cause unexpected economic loss. Therefore, it is vital to evaluate the degradation process of the gear system caused by surface wear propagation in order to make reliable predictive maintenance-based decisions to ensure the safe operation of the gearbox transmission system. The vibration analysis technique is a prevailing tool for rotating machine condition monitoring. However, research on vibration-based gear wear monitoring is relatively rare as the dynamic interactions between gear surface wear and gear system dynamic characteristics would produce complex gear dynamic responses and vibration features. Therefore, this paper presents a novel similarity-based status characterization methodology for gear wear monitoring. In this proposed methodology, a novel gear wear monitoring indicator is developed to evaluate gear

tooth contact characteristics at different wear severities, which could significantly benefit gear systems' health management. The effectiveness of the proposed method for gear wear propagation process monitoring is presented and proven through a series of run-to-failure tests with different lubrications and operational conditions.

Keywords: Gearbox, surface wear, vibration analysis, wear progression, status characteristics.

1 Introduction

Gearbox, a critical component for rotating machinery, has many distinguished merits, such as stable operation quality, high transmission efficiency, and accurate transmission ratio. Thanks to the advantages above, the gearbox is widely used as the transmission system in various heavy industry applications such as vehicles, wind turbines, ships, and helicopters [1, 2]. However, the gearbox often operates in adverse working conditions in industrial practice [3, 4]. The harsh operation conditions make gear wear inevitable during the whole gear's service life [5-7]. When gear wear develops to a certain degree of severity, it can induce severe gear failures such as tooth surface spall and tooth broken, which could destroy the whole gear transmission system and cause unexpected economic loss. Therefore, monitoring and predicting gear wear progression is crucial for the health management of gearbox transmission systems [8].

In practice, the wear debris/particle analysis technique is a prevalent way for gear surface wear evaluation and monitoring. Wear particle concentration has been recognized as an indicator to assess a machine's overall wear/degradation condition. Particle size, distribution, and shape can effectively reveal wear mechanisms [9]. However, wear particle analysis is usually implemented offline, which could be costly and time-consuming. Besides, wear particles cannot directly reveal instant changes in gear dynamic characteristics/features, which have close relationships with the running status of the gearbox. In contrast, compared with wear particle analysis, gear vibration signals reflect instant gear dynamic features when they are measured [10]. Thus, vibration analysis can be utilized for permanent and intermittent

monitoring. Therefore, vibration analysis has the potential to be a more suitable tool for assessing gear wear in real-time.

In general, vibration-based machinery prognostics and health management consist of four critical parts: (1) acquisition of vibration signal; (2) construction of vibration health indicator; (3) division of health stages of the machinery; and (4) remaining useful life (RUL) prediction of the machinery [11], among which the health indicator construction and remaining useful life prediction are two main research objectives. The research for health indicator construction [12, 13] aims to develop health indicators to better reveal the degradation progression, while the research for RUL prediction [14-16] targets to develop regression models to obtain RUL through the established map between the health indicator and RUL, which contributes to scheduling predictive maintenance strategies to ensure a safe and reliable operation of machinery [17]. To the best of our knowledge, most of the existing research for machinery prognostics mainly study either health indicator construction or prediction model due to their research focus differences [18, 19]. Similarly, we merely focus on one of these two objectives. In the process of machinery health management, the health indicator is the prerequisite of machinery prognostics, since the final predicted RUL is obtained by the prediction model through developing a map between the health indicator and RUL [19]. A good health indicator can significantly simplify the prognostic modeling, reduce the computation burdens, and help generate accurate prognostic results. Therefore, this paper focuses on the health indicator construction, and developing health indicators to monitor gear wear propagation is the main research objective of this work. In the following, the current research progresses on vibration-based gear wear monitoring will be reviewed and discussed, from the view of health indicator construction.

Vibration analysis techniques have been well developed and widely applied for monitoring common gear failures, such as gear breakages and gear cracks [20]; in contrast, vibration-based

techniques/indicators for gear wear analysis and monitoring are relatively rare. One reason is that the dynamic interactions between gear surface wear and gear system dynamic characteristics would produce complex gear dynamic responses and vibration features, which brings significant challenges to extracting the corresponding vibration features induced by gear wear and developing specific vibration analysis approaches for wear identification and monitoring [21]. Therefore, it is necessary to develop effective vibration-based techniques for gear wear monitoring, which could bring significant benefits to the health management of gear systems.

Up to date, the existing vibration-based surface wear monitoring techniques are pretty general and limited. For example, the study [22] revealed that gear tooth wear might lead to an amplitude increment of the gear tooth meshing harmonics, and the amplitudes of higher-order gear meshing harmonics are a credible way of detecting incipient uniform wear. Similarly, the magnitude of quefrencies in cepstrum and gear meshing harmonics in the frequency spectrum were utilized in Ref. [23] to evaluate the gear wear process. However, the average engaging tooth profile will continue deviating further from the ideal gear involute profile in the gear wear propagation process, but the changes are not determined in the tooth meshing harmonics. The change behaviors of gear meshing harmonics could vary considerably; besides, some gear meshing harmonics may keep increasing in a certain period, but a decreasing trend occurs in the following duration. Thereby, all the meshing harmonics of gears which have significant energy were considerated in [5], then the sideband ratio (SBR) was extended and modified into two new gear wear monitoring indicators: one is averaged logarithmic ratio (ALR), and the other one is moving averaged logarithmic ratio (mALR). The proposed ALR can be used to indicate the severity of accumulated wear. mALR reflects the instant gear state changes. The performances of the two gear wear indicators were evaluated by two sets of tests that have different initial tooth surfaces. Recently, Ref. [24, 25] applied the modulation signal bispectrum

to vibrations and motor current signals for gear wear monitoring; corresponding experiments validated the effectiveness of the proposed methods.

From the above literature review, it can be seen that most of the exiting techniques for gear wear monitoring are developed based on the general characteristics existing in the time and frequency domains, which might have limited ability to reveal the unique system degradation status caused by gear surface wear propagation progression. Moreover, the distinctive interactions and coupling effects between gear surface wear and dynamic responses make the measured vibrations have significant nonlinear and nonstationary characteristics. The nonlinearity and nonstationarity of vibrations bring considerable challenges to effective gear wear monitoring. Besides, most of the existing techniques are valid for one wear mode. However, multiple wear mechanisms exist and interact with each other during the gear wear progression in industry practices. Consequently, it will lead to the existing techniques losing effectiveness in tracking gear wear propagation in actual industrial scenarios. Therefore, it is vital to develop more reliable and practical methodologies for monitoring and assessing the surface wear progression in gear systems.

With consideration of the nonlinear vibration characteristics induced by the coupling effects between gear surface wear and gear dynamics, the approach of measuring the complexity of gear systems can be an effective and efficient tool to indicate the gear wear process. Thus, this paper proposes a similarity-based status characterization methodology to monitor and assess gear wear propagation. More specifically, the relationships between gear wear tribological features and vibration characteristics tied to unique gear system kinematics are investigated first. Then based on the achieved understanding of gear mechanisms, a novel gear wear indicator is developed to assess the complexity of gear systems caused by gear wear progression. This novel gear wear indicator can effectively reveal the tooth surface degradation

status caused by the gear wear process, providing valuable information to gear systems' health management and bringing significant benefits to industry practice.

To conclude, the main contributions of this paper are summarized as follows:

1) The relationships of gear surface wear, gear dynamics, and vibration characteristics are comprehensively investigated. This investigation reveals the impacts of gear wear progression on vibration characteristics from machine mechanism views, which significantly benefits the health indicator constructions for monitoring gear wear progression.
2) A novel gear wear monitoring indicator is developed based on the analysis of measured vibrations. This novel gear wear indicator can accurately capture the wear-induced morphology characteristics' changes. Moreover, unlike the existing studies, which are effective for one wear mechanism, the novel indicator is valid and effective for multiple gear wear mechanisms.
3) Natural wear propagation tests under different lubrication and operating conditions are arranged to verify the effectiveness of the proposed methodology. Also, comparisons with the traditional indicators are included in this paper to show the proposed indicator's superiority in assessing surface wear propagation progression.

The following sections of this paper are structured as follows: the impacts of gear wear on vibration characteristics and the complexity of gear transmission systems are introduced in Section 2; The proposed similarity-based status characterization methodology for gear wear monitoring is introduced in Section 3; Section 4 demonstrates the superiority of the developed method over traditional indicators/techniques with two kinds of measurements from laboratory gear rig under different lubrication conditions. Conclusions are drawn in Section 5.

2 Wear effects on vibration characteristics

2.1 Relationship between gear wear and vibrations

In general, gear wear progression affects the gear tooth durability in two directions: (1) in the direction normal to the gear tooth surface; gear wear can reduce the gear tooth thickness and introduce geometric deviation from the ideal involute profile, due to sliding motions. It usually is in millimeter-level, which can be called macro-wear; (2) meanwhile, the morphology on gear surface will change significantly during gear wear progression, which tends to be quantified by surface roughness; in general, the surface morphology change is at micrometer-level, called micro-wear [26]. Macro-wear is usually caused by abrasion. In contrast, all gear wear modes involve micro-wear progression, such as abrasion, fatigue pitting, corrosive wear, etc.

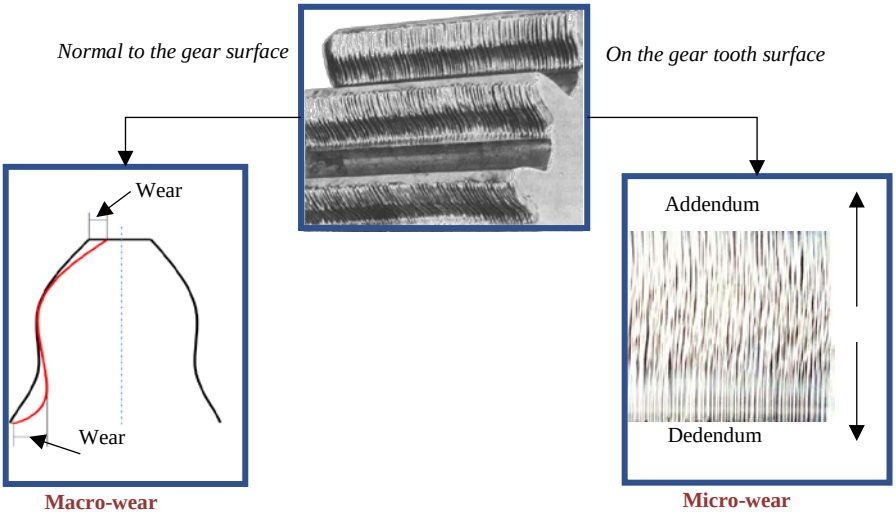

Figure 1 Gear tooth change induced by gear wear progression

In theory, macro-wear is distributed uniformly on each gear tooth, resulting in an increase in gear meshing harmonics [22, 27]. However, in practice, there will be different wear propagation rates exiting among these teeth due to the manufacturing error and lubrication contamination, which brings in differences of geometric deviation to each tooth. During gear wear progression, the dynamic load alternation during the wear process reduces this kind of tooth-to-tooth difference to some extent. The tooth-to-tooth differences conduce the occurrence

and changes of sidebands around gear meshing harmonics [5]. While gear meshing harmonics and their sidebands are the deterministic components of vibrations. That means the macro-wear propagation could lead to a noticeable change in deterministic components signal.

Micro-wear corresponds to the surface morphology change during its progression. In gear's service lifespan, the tooth surface degradation usually involves multi-wear mechanisms [28]. Each wear mechanism can bring noticeable changes to gear surface morphology. Moreover, the dominant wear mechanism might vary due to the alteration of contact pressure distribution, lubrication quantity and quality, operating conditions, and surface roughness [9, 26, 28]. Thus, compared with macro-wear, monitoring the micro-wear progression can provide more reliable and valuable information to the gear system's health management. Therefore, investigating the vibration characteristics, which can reveal micro-wear propagation progression, are vital and deserve more attention from the research community and industry.

Considering its unique characteristics, the micro-wear has negligible effects on the deterministic vibration signal unless it is exceptionally severe like the macro-wear. Thus, it is challenging to develop effective techniques/indicators to extract useful features for tracking micro-wear progression. As for the gear transmission system, there are inevitable sliding motions between the meshing gear pairs. The sliding behaviors and friction on the gear surface asperity contact can produce vibrations. This kind of vibration signal is a random signal, and its nature depends on several factors, such as operation conditions, lubrication status, and micro surface morphology of the gear surface [29]. The progression of gear wear can result in a change of gear asperity contact and affect gear sliding vibration characteristics. Therefore, some recently published research [27, 29] suggests that micro-wear, resulting in tooth surface morphology change, has noticeable effects on the sliding vibration. For instance, as introduced in Ref. [27], the progression of gear wear would cause an increase in surface roughness of the engaging gear pairs; consequently, the magnitude of the sliding vibration will increase

accordingly, as shown in Figure 2. Thus, based on the above discussions and analysis, sliding vibration-based analysis has the potential to be a promising approach for monitoring micro-wear propagation.

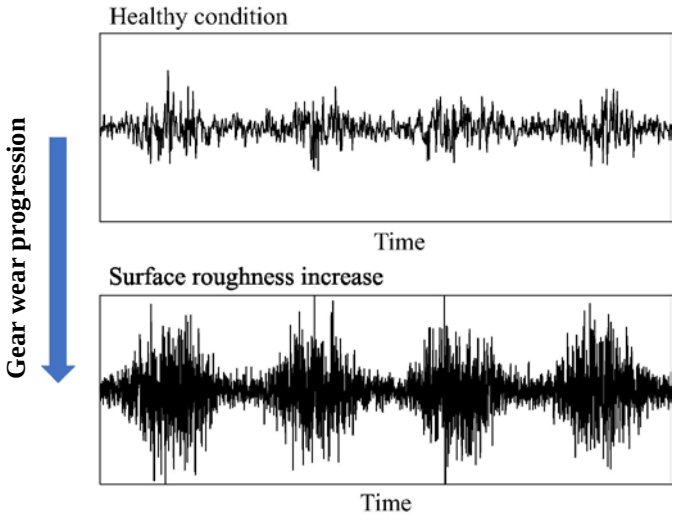

Figure 2 An example to show the connection between the progression of gear wear and sliding vibrations [27]

To conclude, the wear effect on vibration characteristics can be summarized and demonstrated in Figure 3.

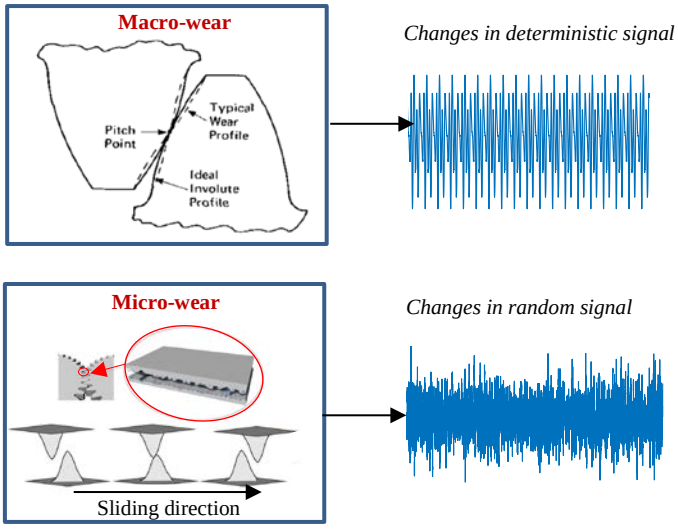

Figure 3 Wear effects on vibration signal: macro-wear and micro-wear

2.2 Extraction of sliding vibrations

Gear surface morphology closely relates to the sliding vibrations, as introduced above; thus, analyzing the wear-induced sliding vibration can significantly benefit the gear wear progression monitoring. However, in the measured vibrations, the dominant components are

deterministic signals generated by the gear meshing and shaft rotating behaviors. Thus, it is necessary to exclude the deterministic components and extract the sliding vibrations from the measured vibrations.

In theory, the measured vibration signal $y(t)$ from gearbox transmission system is the product of convoluting an impulse response signal $h(t)$ and an excitation signal $x(t)$:

$$y(t) = x(t) * h(t) \tag{1}$$

As for the gear transmission system, the dominant excitation signal closely relates to the rotating speed of the input and output shaft and the corresponding drive trains. The main excitation vibration signal usually is composed of discrete frequency components. In addition to the excitation signal (also namely forcing signal), the structural responses of the gearbox, corresponding to the natural frequencies of the system and the impulse responses, also exist in the acquired vibration signal, as less systematic (almost random) vibrations [30]. The discrete/random separation (DRS) algorithm is to explore and investigates the inherent relations of the vibration signal with the delayed version of itself. A high inherent correlation is anticipated between the vibration signal to be analyzed and the delayed version of itself if there is a deterministic vibration signal component in the measurements. In contrast, a low correlation would be expected if the dominant component of the measurement is a random signal. This information can help separate the gear vibration signal's random and deterministic components. Figure 4 shows the calculation procedure of the DRS transfer function.

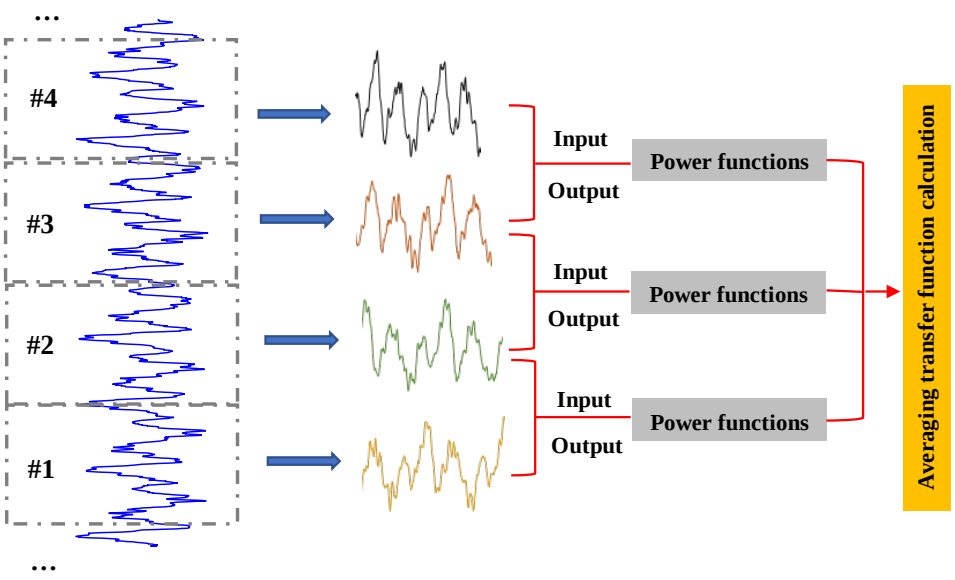

Figure 4 Schematic demonstration of the calculation process of the DRS transfer function [31]

The fundamental theories and equations of the DRS technique are presented as follows. As for the gearbox transmission system, H_1 estimator is used to define its transfer function

$$H_1(f) = G_{xy}(f)/G_{xx}(f) \tag{2}$$

where $G_{xy}(f)$ is the cross-spectrum

$$G_{xy}(f) = \Im\{y(t)\}\Im^*\{x(t)\} \tag{3}$$

and $G_{xx}(f)$ is the auto-spectrum

$$G_{xx}(f) = \Im\{x(t)\}\Im^*\{x(t)\} \tag{4}$$

Note: $\Im$ denotes the Fourier transfer, and the complex conjugate is represented by $*$ in the superscript.

In the DRS's transfer function, the non-delayed vibration signal is defined as the input signal $x(t)$, and its corresponding delayed version is set as the output signal $y(t)$. A process of averaging is implemented to boost the calculation of the transfer function:

$$G_{xy}(f) = \frac{1}{N}\sum_{i=1}^{N} \Im\{y_i(t)\}\Im^*\{x_i(t)\} \tag{5}$$

$$G_{xx}(f) = \frac{1}{N}\sum_{i=1}^{N} \Im\{x_i(t)\}\Im^*\{x_i(t)\} \tag{6}$$

The inverse Fourier transform algorithm helps transfer the achieved transfer function from the domain of frequency to the domain of time:

$$h(t) = \Im^{-1}\{H_1(f)\} \tag{7}$$

The achieved transfer function can help filter the originally measured vibrations. After the filtration, the random components of the measured vibrations can be gained, which contains rich information of the gear surface morphology.

A. Cyclostationarity of vibration caused by gear wear

Through the separation of deterministic and random signals via DRS, the random components of vibrations can be obtained. However, in the random vibrations, the sliding-induced vibrations are still mixed with background noise. Moreover, the energy of sliding vibration is weak, resulting in valuable features easily being submerged into noise. Thus, the random signal after filtering through DRS should be further processed so that the surface morphology-related vibration components (sliding induced vibrations) can be appropriately represented.

The unique gear system kinematics is shown in Figure 5. The periodic gear mesh behavior (in Figure 5(a)) and contact force of engaging gears (in Figure 5(b)) produce a periodic sliding velocity corresponding to the gear mesh frequency, as demonstrated in Figure 5(c). The sliding velocity is zero at the gear pitch line and increases linearly as the gear mesh point departs from the pitch line. The varying sliding velocity and periodic contact force could generate an amplitude modulation to the sliding vibrations, as shown in Figure 5(d). The carrier signal is the random vibration from the engaging gears' surface asperity contacts. And the amplitude modulating frequency corresponds to the gear mesh behaviors. Thus, the micro surface wear should be correlated to the second-order cyclostationarity at the gear mesh cyclic frequency. In other words, second-order cyclostationary (CS2) phenomena exist in the sliding induced random signal. Therefore, the cyclostationary analysis tools have the potential to benefit micro-wear monitoring.

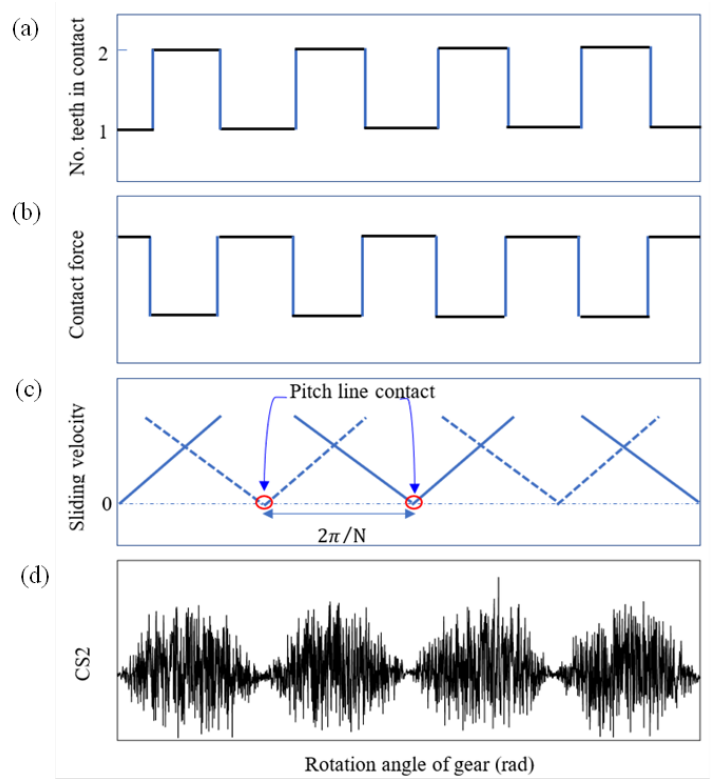

Figure 5 Second-order cyclostationary (CS2) signal generation from periodic contact force and the meshing gear sliding velocity; (a) the number of tooth pairs in contact; (b) approximate contact force; (c) approximate sliding velocity; (d) possible amplitude-modulated random signal (CS2) generated from varying sliding velocity (N = number of teeth on the gear) [29].

In theory, the second-order moment of cyclostationarity of measured vibration signal $z(x)$ can be recognized as an instantaneous autocorrelation function with T cyclic period [32]:

$$R_{xx}(t,\tau) = R_{xx}(t+T,\tau) = E\{z(t+\tau/2)z(t-\tau/2)\} \tag{8}$$

where $E\{\cdot\}$ denotes the ensemble average operator; τ is the time-lag. The autocorrelation function's Fourier coefficients correspond to the cyclic autocorrelation function, which are:

$$R_{xx}(\tau,\alpha) = \int R(t,\tau)e^{-j2\pi\alpha t}\,dt \tag{9}$$

where the cyclic frequency defines as α. In Eq. (9), it can be seen that the cyclic autocorrelation function denotes the Fourier coefficients of α for a time-lag signal $R(t,\tau)$. Based on Eq. (8), the spectral correlation, one of the powerful CS2 analysis tools, can be calculated as follows [33]:

$$S(\alpha, f) = \int R_{xx}(\tau, \alpha) e^{-j2\pi f \tau} d\tau$$
$$= \iint R(t, \tau) e^{-j2\pi(\alpha t + f\tau)} dt d\tau \quad (10)$$

Superior to spectral correlation, spectral coherence can magnify the weak cyclostationarity of the measured signal [34]. The spectral coherence is achieved through normalizing the spectral correlation; spectral coherence can reveal the level of modulation with cyclic frequency α and a carrier with spectral frequency f as follows:

$$\gamma(\alpha, f) = S(\alpha, f) / \sqrt{S(0, f) S(0, f - \alpha)} \quad (11)$$

As for the gear case, due to the unique kinematics of the gear transmission system, the gear mesh cyclic frequencies contain rich surface morphology information, as shown in Figure 6 (limited gear mesh cyclic harmonics are presented for demonstration purposes). Thus, the slices of gear mesh cyclic frequencies can be used for monitoring the gear wear progression.

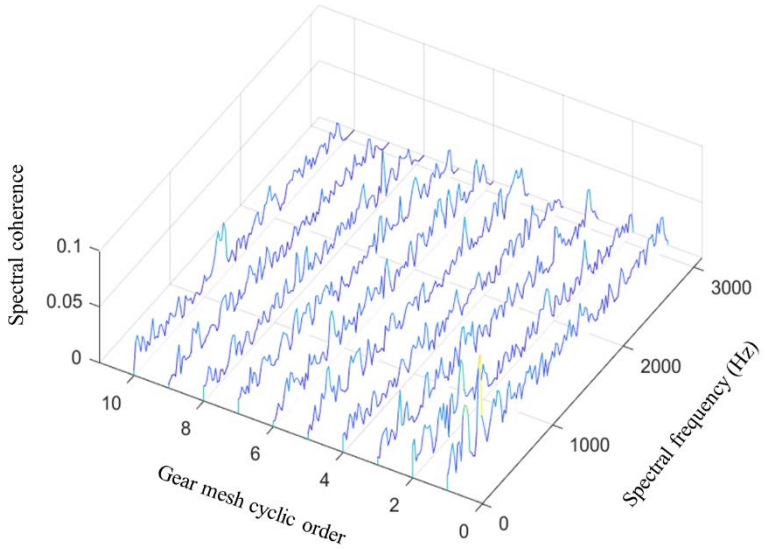

Figure 6 Spectral distribution at the gear mesh cyclic order (the first ten)

Even though the slices of gear mesh cyclic frequencies contain rich surface degradation information, it is challenging to indicate/interpret the gear system degradation status by directly observing the spectral coherence maps. Also, the slices of gear mesh cyclic frequencies could not indicate the wear severity intuitively. To address this issue, the slices of gear mesh cyclic

frequencies can be treated as data from multiple pseudo sources. Inspired by the multivariate dispersion entropy [35], a novel gear wear monitoring indicator employing the gear mesh cyclic frequencies as pseudo sources of interest is established. The developed similarity-based status characterization gear wear monitoring methodology will be introduced in Section 3.

3 Proposed methodology for gear wear monitoring

In this section, the proposed similarity-based status characterization methodology, which can comprehensively represent the gear system degradation behaviors caused by surface wear progression, is presented.

The calculation procedures of the developed gear wear monitoring indicator are presented as follows:

Step 1: The acquired vibration signal from the gearbox system is denoted as $y(t)$. Following the Eqs. (1-7), the separation filter is constructed as

$$(|W(f)|^2 \rho N/2)/(|W(f)|^2 \rho N/2 + 1) \tag{12}$$

where N represents the transform size. The applied Fourier transform window is denoted as $W(f)$, it has been mapped to a scale in the frequency domain whose maximum value is 1. In addition, $\rho =$ SNR (signal-to-noise ratio). The random signal $y_r(t)$ is obtained through implementing Eqs. (1-7) and Eq. (12).

Step 2: Autocorrelation function $R_{y_r y_r}(t, \tau)$ of $y_r(t)$ is calculated, followed by the two-dimensional Fourier transformation of $R_{y_r y_r}(t, \tau)$. At last, the spectral coherence $\gamma_{y_r y_r}(\alpha, f)$ is obtained through:

$$\gamma_{y_r y_r}(\alpha, f) = \iint R_{y_r y_r}(t, \tau) e^{-j2\pi(\alpha t + f\tau)} dt d\tau / \sqrt{S(0, f) S(0, f - \alpha)} \tag{13}$$

Based on the analysis of Figure 5, the signal at the gear mesh cyclic harmonics, which are signals at $\alpha = f_{\mathrm{GM}^{q\mathrm{th}}}$ ($\mathrm{GM}^{q\mathrm{th}}$ denotes the qth gear mesh harmonic), closely related to the gear

surface morphology. Thus, $\gamma_{y_r y_r}(\alpha, f)$ at slices of gear mesh cyclic harmonics are extracted from the bi-spectral maps of $\gamma_{y_r y_r}(\alpha, f)$ for further analysis.

Step 3: Normalize the extracted signals at multiple slices of gear mesh cyclic harmonics from $\gamma_{y_r y_r}(\alpha, f)$. The extracted signals are denoted as $\boldsymbol{\mathcal{M}} = \{\mathcal{M}_{k,h}\}_{k=1,2,\cdots,n}^{h=1,2,\cdots,N}$, where N is the signal length at each cyclic harmonics of gear mesh, and n is the number of gear mesh cyclic harmonics to be considered. Then the signals $\boldsymbol{\mathcal{M}} = \{\mathcal{M}_{k,h}\}_{k=1,2,\cdots,n}^{h=1,2,\cdots,N}$ are mapped into a new signal $\mathbf{G} = \{g_{k,h}\}_{k=1,2,\cdots,n}^{h=1,2,\cdots,N}$ (whose value is between 0 and 1) through the normal cumulative distribution functions [36] as

$$g_{k,h} = 1/\left(\sigma_k\sqrt{2\pi}\right)\int_{-\infty}^{x_{k,h}} e^{\frac{-(t-\mu_k)^2}{2{\sigma_k}^2}}dt \tag{14}$$

where σ and μ denote the standard deviation and mean of gear mesh cyclic harmonic signals, respectively, this normalization process will increase the SNR of the signal, which can help improve its diagnosis capability. Also, a linear transform $z_{k,h} = \mathbf{R}\left(c \cdot g_{k,h} + 0.5\right)$ is utilized to re-map the signal from **G** to **Z** (from 1 to c); **R** is the rounding function.

Step 5: The signal **Z** is reconstructed based on the multivariate embedding theory:

$$\begin{aligned} Z_m(j) = \big[&z_{1,j}, z_{1,j+d_1}, \cdots, z_{1,j+(m_1-1)d_1}, \\ &z_{2,j}, z_{2,j+d_2}, \cdots, z_{2,j+(m_2-1)d_2}, \cdots, \\ &z_{n,j}, z_{n,j+d_n}, \cdots, z_{p,j+(m_n-1)d_n}\big] \end{aligned} \tag{15}$$

where $j \in [1, N-(m-1)d]$, $m = [m_1, m_2, \cdots, m_n]$ represents embedding dimension and $\lambda = [\lambda_1, \lambda_2, \cdots, \lambda_n]$ represents time delay.

Step 6: For every $Z_m(j)$, all possible combinations of m elements in $Z_m(j)$, termed $\phi_{q,l}(j)$ $(q \in [1, C_m^{mn}], l \in [1, m])$, have been created, where the C_m^{mn} is the total number of all combinations of mn numbers with length m.

Step 7: Each $\phi_{q,l}(j)$ is mapped to a pattern $\pi_{v_0 v_1 \cdots v_{m-1}}(v = 1,2,\cdots,c)$, where $\phi_{q,1}(j) = v_0$, $\phi_{q,2}(j) = v_1$, $\cdots$, $\phi_{q,l}(j) = v_{m-1}$. Since $\pi_{v_0 v_1 \cdots v_{m-1}}$ has m digits, and each m is with c classes; thus, a total c^m patterns are here. The total number of combinations of each $Z_m(j)$ is C_m^{mn}. Therefore, as for the n channel data, there are a total of $[N-(m-1)d]C_m^{mn}$ patterns.

Step 8: The probability of each pattern is [37]:

$$p\left(\pi_{v_0 v_1 \cdots v_{m-1}}\right) = \frac{Number\left(\pi_{v_0 v_1 \cdots v_{m-1}}\right)}{(N-(m-1)d)C_m^{mn}} \tag{16}$$

where $Number$ in Eq. (16) demotes the number of $\pi_{v_0 v_1 \cdots v_{m-1}}$ in $\phi_{q,l}(j)$.

Step 9: At last, based on the theory of Shannon entropy, the gear wear monitoring indicator DE_{MC} is calculated by

$$DE_{MC} = -\sum_{\pi=1}^{c^m} p\left(\pi_{v_0 v_1 \cdots v_{m-1}}\right) \ln p\left(\pi_{v_0 v_1 \cdots v_{m-1}}\right) \tag{17}$$

With the developed novel gear wear monitoring indicator DE_{MC}, the gear system degradation behaviors can be revealed (as shown in Figure 7), and the wear progression can be assessed. The unique advantages of the developed novel gear wear monitoring indicator (over traditional indicators) are summarized as follows:

- Surface morphology-related sliding induced vibration is involved in the novel gear wear indicator; thus, it has a better ability to track and assess the surface degradation process caused by gear wear propagation over other conventional but prevalent indicators, e.g., cyclostaionary indicators, statistical indexes, and gear meshing harmonics.
- The novel gear wear indicator is valid in tracking gear wear progression for multiple wear mechanisms. The developed gear wear indicator focuses on the vibration characteristics caused by micro surface morphology alternation, and all gear modes involve surface morphology change; thus, it is still effective in tracking gear wear progression, even though

multiple wear mechanisms exist or the dominant wear mode varies during the gear progression process.

- Multiple slices of gear meshing cyclic harmonics are considered, which brings more comprehensive information to describe the surface degradation process, compared with using a single gear mesh cyclic harmonic.

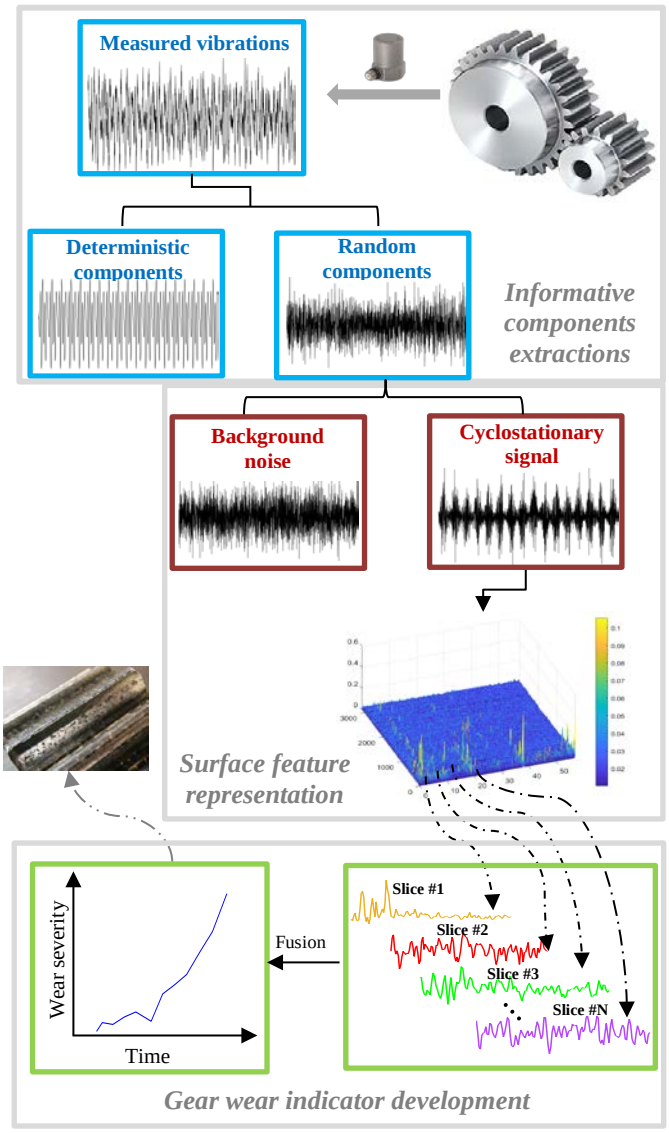

Figure 7 Calculation procedure of the developed similarity-based status characterization gear wear monitoring approach

The effectiveness of the developed similarity-based status characterization gear wear monitoring methodology will be verified using the run-to-failure tests with different operating

conditions under different lubrication conditions, as introduced in the following section: Section 4.

4 Experiment

A series of gear run-to-failure tests were designed and conducted on the test rig, and different lubrication conditions were involved, that is, with and without lubricating oil. The tested gearbox rig's schematic diagram is presented in Figure 8. The tested gearbox test rig is composed of meshing gear pairs, casing, shafts, motor, support bearings, couplings, and a brake. There are two high-resolution encoders that are placed on the free end of connection shafts. The encoder signals and vibration signals were acquired at 102,400 Hz sampling frequency for 15s. The gear surface morphology is revealed by a moulding technique. Moreover, a microscope was applied to scan the collected mould to obtain the 3D surface images of the gear surface morphology (as demonstrated in Figure 9), and the tribological features were calculated, such as the tooth surface roughness S_a. The gear tooth surface roughness can be applied to help validate the effectiveness of the proposed methodology for evaluating the system degradation severity during the gear wear propagation progression.

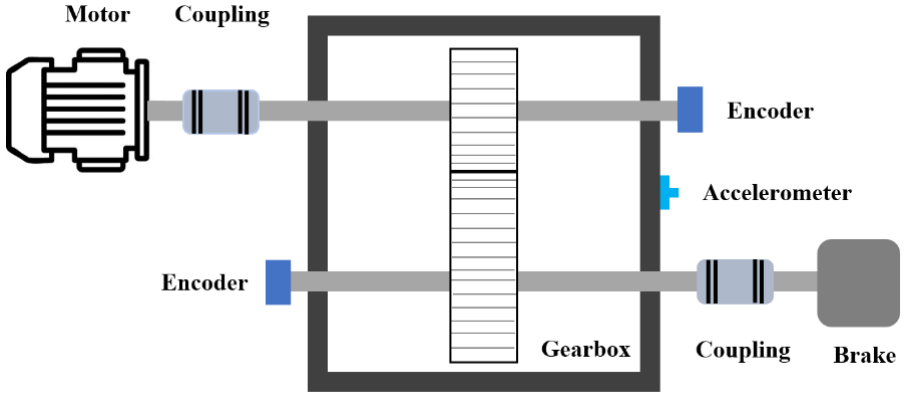

Figure 8 Gearbox test rig schematic diagram

Figure 9 Demonstration of the process of obtaining the surface morphology feature during the gear wear propagation

4.1 Gear wear progression monitoring with lubrication oil

The gearbox was first run with lubricating oil. Four endurance tests were arranged with 25 Nm applied load. The operating speeds of four tests were set as 10 Hz, 15 Hz, 20 Hz, and 25 Hz, respectively. In this section, to avoid repetition, only the endurance test with a 20 Hz rotating speed will be used to demonstrate the implementation procedures of the developed similarity-based status characterization gear wear monitoring methodology. The final analysis results of other endurance tests will be summarized in a table directly.

From the duplicated gear surface morphology, it reveals that the main mechanism of gear wear in the lubricated test (20 Hz) is gear fatigue pitting, as shown in Figure 10. The same dominant mechanism was observed in other endurance tests (with lubrications).

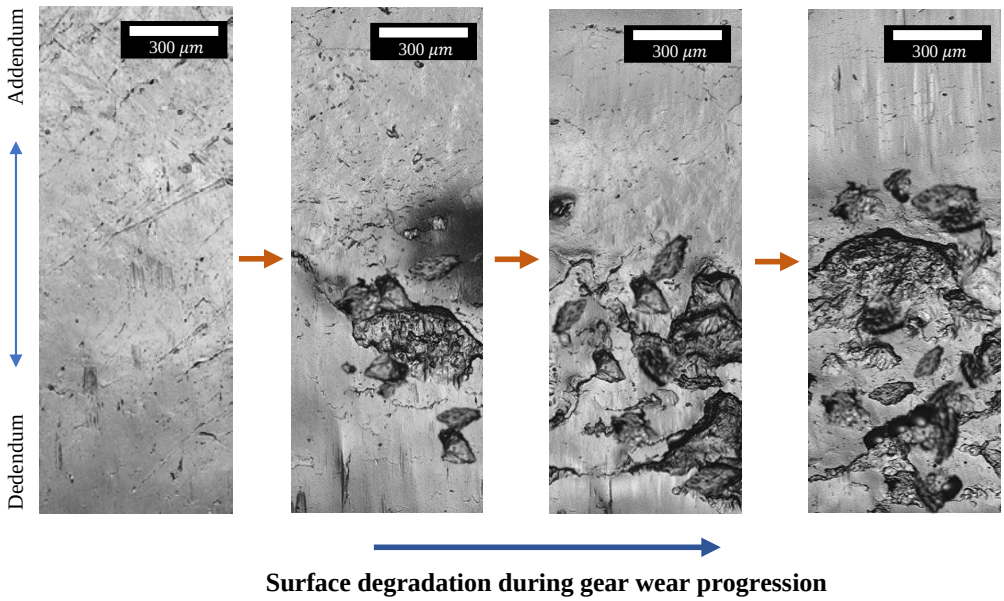

Figure 10 Driving gear tooth surface degradation progression induced by gear wear: one specific location

The developed similarity-based status characterization methodology is applied to this endurant test (20 Hz) to monitor and assess the gear surface degradation characteristics with lubricating oil. Moreover, to quantitively evaluate the degradation progression on the gear surface, surface roughness (arithmetical mean height S_a) is selected as the feature of the microsurface morphology to reflect the gear wear severity. S_a will be applied to evaluate the effectiveness of the novel indicator DE_{MC} for monitoring gear wear, obtained from the proposed similarity-based status characterization methodology.

The trend of the proposed gear surface wear indicator DE_{MC} is shown in Figure 11(a) (blue colored line). The R-squared analysis tool is utilized in this paper to demonstrate and quantify the performance of the proposed health indicator DE_{MC} in monitoring and evaluating gear wear progression. As a statistical measure of fit, the R-squared indicates how much variation of a dependent variable is explained by the independent variable(s) in a regression model. The two variables of R-squared are set as the proposed health indicator DE_{MC} and surface roughness S_a. Thus, the R-squared contributes to revealing and quantifying the internal relationship between DE_{MC} and S_a. The R-squared analysis result is shown in Figure 11(b). From Figure 11(b), a linear regression model is applicable, and there is a high correlation coefficient value, which is $R^2 = 0.9659$. It indicates a strong linear relationship between DE_{MC} and S_a. Therefore, the developed gear wear monitoring indicator DE_{MC} is proved to have an outstanding performance in monitoring gear wear propagation progression.

Meanwhile, several conventional indicators are applied in this paper for comparison purposes, such as the typical cyclostationarity indicators, namely ICS2 [28] and RCC [38, 39], and some other traditional indicators: kurtosis, RMS, and harmonics of gear meshing. Moreover, the R-squared is utilized as the tool to quantify the performance of these indicators in monitoring and assessing the process of gear wear progression. The analysis and comparison results are introduced in Table 1.

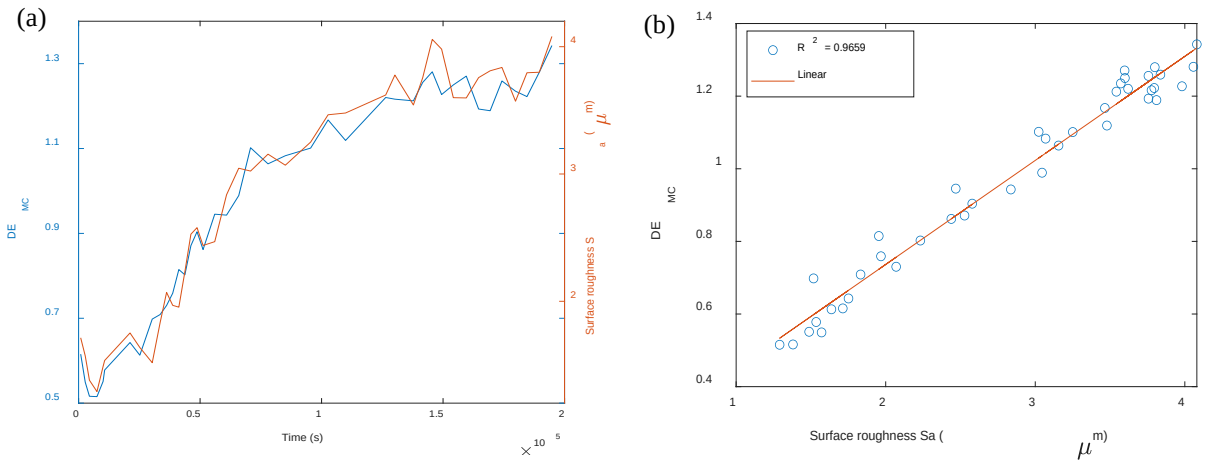

Figure 11 DE_{MC} in monitoring gear wear progression: with lubrication

Table 1 Gear wear monitoring: with lubrication

Indicator	Correlation coefficient with surface roughness S_a: R^2			
	Test: 20 Hz	Test: 10 Hz	Test: 15 Hz	Test: 25 Hz
DE_{MC}	**0.9659**	**0.9543**	**0.9478**	**0.9602**
ICS2	0.8134	0.7998	0.8248	0.8546
RCC	0.7546	0.7864	0.7732	0.8423
RMS (raw vibration signal)	0.7124	0.7269	0.7789	0.7764
RMS (residual vibration signal)	0.7824	0.7745	0.7652	0.8251
Kurtosis (raw vibration signal)	0.7205	0.7452	0.5489	0.6548
Kurtosis (residual vibration signal)	0.0714	0.0981	0.1288	0.2365
1st harmonic of gear meshing	0.0970	0.1147	0.0647	0.0589
2nd harmonic of gear meshing	0.0470	0.0579	0.0892	0.0546

The comparison results with 20 Hz are discussed as follows. As shown in Table 1, the maximal value of the correlation coefficient of other indicators is $R^2 = 0.8134$, which is achieved by the second-order cyclostationarity (CS2) indicator ICS2. Likewise, RCC, another CS2 indicator, is also highly correlated to the gear surface roughness. It implies that the vibration-based cyclostationary analysis approach has the potential to be a good tool to monitor the process of gear wear propagation; nevertheless, it needs to select an informative frequency

band first (as introduced in [27]). However, neither of the above-mentioned cyclostationary indicators has a higher R-squared value compared with the proposed indicator DE_{MC}. Therefore, the proposed indicator has a better performance in evaluating gear wear progression than other conventional indicators, and its unique advantage has been quantified and proved by the R-squared analysis.

In addition, RMSs of the raw vibration signal and residual vibration signal show high connections with the gear wear progression, which are $R^2 = 0.7124$ and $R^2 = 0.7824$, respectively. It indicates that the surface wear process can cause energy changes in the vibration signal. However, the kurtosis of the measured vibrations presents a correlation coefficient with a low value compared with the progression of gear wear propagation. The same phenomenon occurs in the harmonics of gear meshing. It means that kurtosis and harmonics of gear meshing might not be reliable indexes for monitoring and assessing gear surface degradation severity during the process of gear wear propagation.

Similar comparison results are achieved for the other endurance tests, with 10 Hz, 15 Hz, and 25 Hz. It means the developed gear wear indicator DE_{MC} is robust for tracking the progression of gear surface wear under lubrication conditions.

To conclude, as demonstrated in the comparison analysis with the above-mentioned conventional health indicators, it can be seen that the proposed gear wear indicator DE_{MC} has the best capability and performance; thus, it can be serviced as a robust tool for evaluating the degradation severity of gear systems caused by surface wear propagation progression.

4.2 Gear wear progression monitoring without lubrication oil

Another kind of gear run-to-failure test was conducted to validate the effectiveness and capability of the proposed gear wear indicator in assessing the progression of surface wear. It is executed without lubrication oil. In these dry endurance tests, the operating speeds were set

as 5 Hz, 8 Hz, 10 Hz, and 15 Hz, and the applied load for the dry tests was set as 10 Nm. Same to Section 4.1, the 10 Hz case was used for demonstration purposes.

Gears are run under lubricated conditions in the majority of industrial applications. However, there are several specific applications that the gears have to run in dry, such as nuclear, aerospace, servo-mechanisms, food processing, and in-space [40]. To prove the excellent applicability of the proposed gear wear monitoring indicator (even for some extreme situations), the dry test was arranged. In addition, another purpose of this dry test is to help generate other wear mechanisms so that the ability of the proposed health indicator for monitoring and assessing gear wear progression with different mechanisms can be examined and proved. In general, as for the fully lubricated gear system, the dominant wear mechanism is fatigue pitting, as introduced in Section 4.1. Unlike the lubricated gear system, the dominant gear wear mechanism of the dry test is abrasive wear, see Figure 12.

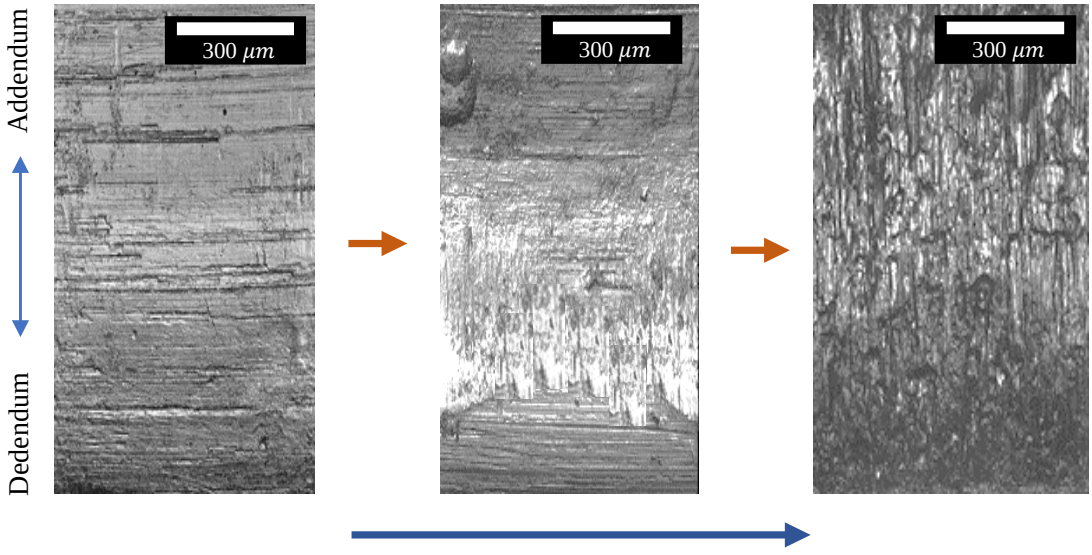

Figure 12 Driving gear surface degradation progression: one specific location

Likewise, the proposed gear wear indicator DE_{MC} is used here to monitor and assess the gear surface wear propagation (see Figure 13(a)), also the corresponding correlation analysis with surface roughness of gear S_a is conducted (see Figure 13(b)). A high correlation coefficient, that is $R^2 = 0.9651$, suggests that the proposed gear wear monitoring indicator has an

outstanding performance and capability in assessing surface degradation characteristics and behaviors during the progression of gear wear propagation, even though the lubrication conditions and wear mechanisms have changed significantly. It proves that the proposed gear wear indicator DE_{MC} is a reliable and robust indicator for gear wear monitoring, which can significantly benefit the research community and industry practices.

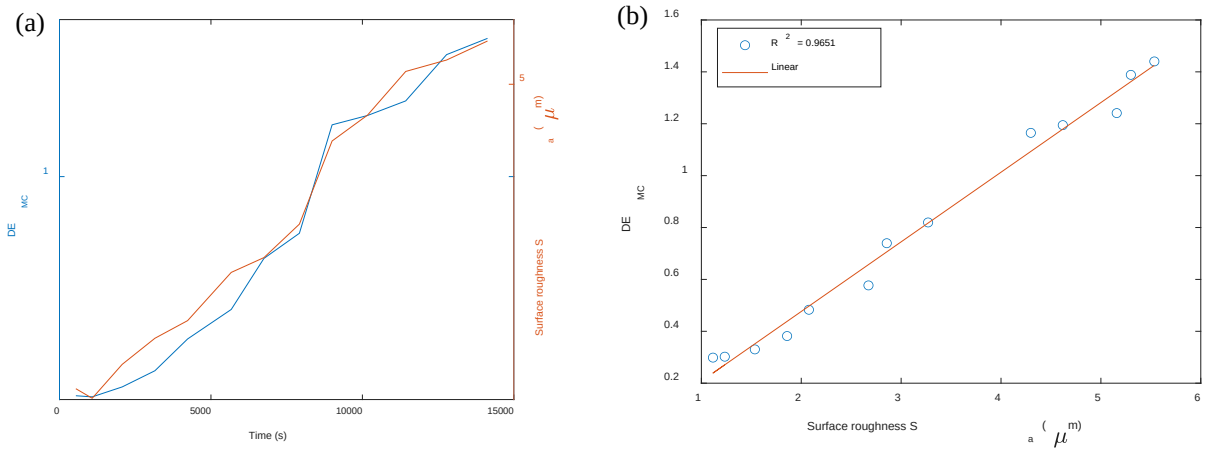

Figure 13 DE_{MC} in monitoring gear wear progression: without lubrication

Similar to the lubricated test, some conventional indicators are applied here to implement the relevant comparisons. The comparison analysis results are summed up in Table 2. As shown in Table 2, it can be seen that the CS2 indicators that are RCC and ICS2 show some correlations or connections with the degradation characteristics of the gear surface, which are indicated and quantified by R-squared analysis with the gear surface roughness S_a. Nevertheless, the effectiveness and performance of CS2 indicators are still inferior to the proposed gear wear indicator DE_{MC}. The RMS indicator (both the raw and residual vibration signals) correlates with gear surface roughness increases to some extent compared with the test with lubrication oil. The possible reason is that gear surface morphology changes much more significantly without lubrication oil, which results in a significant vibration signal energy change. In addition, the correlation between kurtosis and surface morphology features becomes very much higher, compared with the test with lubricating oil. This is owning to a much rougher gear engaging surface involved in the progression of the gear wear propagation without lubricating oil, as

presented in Figure 12. The gear meshing harmonics performance in gear wear monitoring is still not good, which means that it might not be a suitable index for assessing the changes of gear surface micro-features.

Table 2 Gear wear monitoring: without lubrication

Indicator	Correlation coefficient with surface roughness S_a: R^2			
	Test: 10 Hz	Test: 5 Hz	Test: 8 Hz	Test: 15 Hz
$\mathbf{DE_{MC}}$	**0.9651**	**0.9643**	**0.9701**	**0.9548**
ICS2	0.7634	0.7852	0.7796	0.7689
RCC	0.7586	0.7748	0.7721	0.7542
RMS (raw vibration signal)	0.7835	0.8201	0.8001	0.7985
RMS (residual vibration signal)	0.8167	0.8321	0.8054	0.8251
Kurtosis (raw vibration signal)	0.7995	0.7745	0.7689	0.7922
Kurtosis (residual vibration signal)	0.8320	0.8452	0.8321	0.8296
1st harmonic of gear meshing	0.2293	0.3248	0.3165	0.2871
2nd harmonic of gear meshing	0.3434	0.4528	0.2674	0.3859

To sum up, when meshing gear pairs operate without lubricating oil, the dominant mechanism of gear wear has changed. Nevertheless, the proposed gear wear indicator DE_{MC} still has an outstanding performance in assessing the propagation of gear wear; therefore, it is a reliable and robust health indicator for monitoring and evaluating gear system degradation status during surface wear propagation.

5 Conclusion and future work

Surface wear is an inevitable phenomenon during the gear system's lifespan. Also, the dominant wear modes keep changing in the process of gear wear propagation. The propagation of gear wear can lead to severe failure modes. Therefore, it is vital to evaluate the process of gear wear propagation. However, the dynamic interactions between gear wear and gear system

dynamics would produce complex vibration features, resulting in rare vibration-based techniques/indicators being developed for tracking gear wear progression. In this paper, a novel similarity-based status characterization methodology is developed to evaluate the gear surface degradation behaviors. In the proposed methodology, a novel gear wear monitoring indicator DE_{MC} is developed, which can evaluate the gear wear severity, even though different dominant wear mechanisms and lubrication conditions are present. Moreover, comparison analyses with conventional indices were implemented to prove the superiority and advantage of the proposed gear wear indicator in assessing gear wear severity. With the help of R-squared analysis, the correlation analysis quantifiably shows the excellent performance of the proposed gear wear indicator over conventional indicators. Therefore, the developed indicator DE_{MC} is a valuable and reliable tool for non-destructive monitoring and evaluating the degradation status of gear transmission systems induced by the propagation of gear wear in industry practices. Also, the developed gear wear indicator is an online technique, and it can help significantly save labor costs and provide real-time gear system degradation status to the analyst. Accurately assessing the system health status through DE_{MC} could benefit the gear system health management, which is of great importance for various industries. In our future work, prediction models or algorithms to accurately predict the remaining useful life (under surface wear progression) using the developed gear wear monitoring indicator will be studied for the gear transmission system.

References

[1] K. Feng, J.C. Ji, Q. Ni, A novel adaptive bandwidth selection method for Vold–Kalman filtering and its application in wind turbine planetary gearbox diagnostics, Structural Health Monitoring, (2022) 14759217221099966.
[2] H. Li, C.-G. Huang, C. Guedes Soares, A real-time inspection and opportunistic maintenance strategies for floating offshore wind turbines, Ocean Engineering, 256 (2022) 111433.

[3] H.R.F. Fotso, C.V.A. Kazé, G.D. Kenmoé, Real-time rolling bearing power loss in wind turbine gearbox modeling and prediction based on calculations and artificial neural network, Tribology International, 163 (2021) 107171.
[4] J. Zheng, J. Ji, S. Yin, V.-C. Tong, Internal loads and contact pressure distributions on the main shaft bearing in a modern gearless wind turbine, Tribology International, 141 (2020) 105960.
[5] C. Hu, W.A. Smith, R.B. Randall, Z. Peng, Development of a gear vibration indicator and its application in gear wear monitoring, Mechanical Systems and Signal Processing, 76-77 (2016) 319-336.
[6] J. Lin, C. Teng, E. Bergstedt, H. Li, Z. Shi, U. Olofsson, A quantitatively distributed wear-measurement method for spur gears during micro-pitting and pitting tests, Tribology International, 157 (2021) 106839.
[7] H. Liu, H. Liu, C. Zhu, J. Tang, Study on gear contact fatigue failure competition mechanism considering tooth wear evolution, Tribology International, 147 (2020) 106277.
[8] K. Feng, P. Borghesani, W.A. Smith, R.B. Randall, Z.Y. Chin, J. Ren, Z. Peng, Vibration-based updating of wear prediction for spur gears, Wear, 426-427 (2019) 1410-1415.
[9] B. Bhushan, Modern tribology handbook, two volume set, CRC Press, 2000.
[10] Y. Chen, M. Rao, K. Feng, M.J. Zuo, Physics-Informed LSTM hyperparameters selection for gearbox fault detection, Mechanical Systems and Signal Processing, 171 (2022) 108907.
[11] Y. Lei, N. Li, L. Guo, N. Li, T. Yan, J. Lin, Machinery health prognostics: A systematic review from data acquisition to RUL prediction, Mechanical Systems and Signal Processing, 104 (2018) 799-834.
[12] Y. Li, S. Wang, Y. Yang, Z. Deng, Multiscale symbolic fuzzy entropy: An entropy denoising method for weak feature extraction of rotating machinery, Mechanical Systems and Signal Processing, 162 (2022) 108052.
[13] C.J. Li, J.D. Limmer, Model-based condition index for tracking gear wear and fatigue damage, Wear, 241 (2000) 26-32.
[14] Y. Song, S. Gao, Y. Li, L. Jia, Q. Li, F. Pang, Distributed Attention-Based Temporal Convolutional Network for Remaining Useful Life Prediction, IEEE Internet of Things Journal, 8 (2021) 9594-9602.
[15] W. Yu, I.I.Y. Kim, C. Mechefske, An improved similarity-based prognostic algorithm for RUL estimation using an RNN autoencoder scheme, Reliability Engineering & System Safety, 199 (2020) 106926.
[16] C.-G. Huang, H.-Z. Huang, W. Peng, T. Huang, Improved trajectory similarity-based approach for turbofan engine prognostics, Journal of Mechanical Science and Technology, 33 (2019) 4877-4890.
[17] Y. Li, Y. Song, L. Jia, S. Gao, Q. Li, M. Qiu, Intelligent Fault Diagnosis by Fusing Domain Adversarial Training and Maximum Mean Discrepancy via Ensemble Learning, IEEE Transactions on Industrial Informatics, 17 (2021) 2833-2841.
[18] M.M. Manjurul Islam, A.E. Prosvirin, J.-M. Kim, Data-driven prognostic scheme for rolling-element bearings using a new health index and variants of least-square support vector machines, Mechanical Systems and Signal Processing, 160 (2021) 107853.
[19] Q. Ni, J. Ji, K. Feng, Data-driven prognostic scheme for bearings based on a novel health indicator and gated recurrent unit network, IEEE Transactions on Industrial Informatics, (2022) 1-1.
[20] K. Feng, K. Wang, Q. Ni, M.J. Zuo, D. Wei, A phase angle based diagnostic scheme to planetary gear faults diagnostics under non-stationary operational conditions, Journal of Sound and Vibration, 408 (2017) 190-209.
[21] H. Ding, A. Kahraman, Interactions between nonlinear spur gear dynamics and surface wear, Journal of Sound and Vibration, 307 (2007) 662-679.

[22] R.B. Randall, A New Method of Modeling Gear Faults, Journal of Mechanical Design, 104 (1982) 259-267.
[23] S. Ziaran, R. Darula, Determination of the State of Wear of High Contact Ratio Gear Sets by Means of Spectrum and Cepstrum Analysis, Journal of Vibration and Acoustics, 135 (2013).
[24] R. Zhang, F. Gu, H. Mansaf, T. Wang, A.D. Ball, Gear wear monitoring by modulation signal bispectrum based on motor current signal analysis, Mechanical Systems and Signal Processing, 94 (2017) 202-213.
[25] R. Zhang, X. Gu, F. Gu, T. Wang, A.D. Ball, Gear wear process monitoring using a sideband estimator based on modulation signal bispectrum, Applied Sciences, 7 (2017) 274.
[26] A.T. Committee, Appearance of gear teeth: Terminology of wear and failure, American Gear Manufacturers Association, 1995.
[27] K. Feng, W.A. Smith, P. Borghesani, R.B. Randall, Z. Peng, Use of cyclostationary properties of vibration signals to identify gear wear mechanisms and track wear evolution, Mechanical Systems and Signal Processing, 150 (2021) 107258.
[28] K. Feng, W.A. Smith, R.B. Randall, H. Wu, Z. Peng, Vibration-based monitoring and prediction of surface profile change and pitting density in a spur gear wear process, Mechanical Systems and Signal Processing, 165 (2022) 108319.
[29] Y. Yang, W.A. Smith, P. Borghesani, Z. Peng, R.B. Randall, Detecting changes in gear surface roughness using vibration signals, Acoustics 2015 Hunter Valley, (2015) 1-10.
[30] K. Mendrok, K. Dziedziech, P. Kurowski, Detection of structural abnormality of industrial rotary machine using DRS-aided operational modal analysis, Measurement, 164 (2020) 108098.
[31] K. Feng, J.C. Ji, Y. Li, Q. Ni, H. Wu, J. Zheng, A novel cyclic-correntropy based indicator for gear wear monitoring, Tribology International, 171 (2022) 107528.
[32] Z. Chen, A. Mauricio, W. Li, K. Gryllias, A deep learning method for bearing fault diagnosis based on Cyclic Spectral Coherence and Convolutional Neural Networks, Mechanical Systems and Signal Processing, 140 (2020) 106683.
[33] R.B. Randall, J. Antoni, S. Chobsaard, The relationship between spectral correlation and envelope analysis in the diagnostics of bearing faults and other cyclostationary machine signals, Mechanical Systems and Signal Processing, 15 (2001) 945-962.
[34] J. Antoni, G. Xin, N. Hamzaoui, Fast computation of the spectral correlation, Mechanical Systems and Signal Processing, 92 (2017) 248-277.
[35] H. Azami, A. Fernández, J. Escudero, Multivariate Multiscale Dispersion Entropy of Biomedical Times Series, Entropy, 21 (2019).
[36] J. Zheng, H. Pan, Use of generalized refined composite multiscale fractional dispersion entropy to diagnose the faults of rolling bearing, Nonlinear Dynamics, 101 (2020) 1417-1440.
[37] M. Rostaghi, H. Azami, Dispersion Entropy: A Measure for Time-Series Analysis, IEEE Signal Processing Letters, 23 (2016) 610-614.
[38] P. Borghesani, P. Pennacchi, S. Chatterton, The relationship between kurtosis- and envelope-based indexes for the diagnostic of rolling element bearings, Mechanical Systems and Signal Processing, 43 (2014) 25-43.
[39] Q. Ni, J.C. Ji, K. Feng, B. Halkon, A novel correntropy-based band selection method for the fault diagnosis of bearings under fault-irrelevant impulsive and cyclostationary interferences, Mechanical Systems and Signal Processing, 153 (2021) 107498.
[40] D. Walton, A.J. Goodwin, The wear of unlubricated metallic spur gears, Wear, 222 (1998) 103-113.